Identification of Drag Force Point for Small Scale Fixed-Wing Type UAV

Nur Shafa' Darmawan
Faculty of Engineering
Universiti Pertahanan Nasional Malaysia
Kuala Lumpur, Malaysia
nurshafadarmawan@gmail.com

Syed Mohd Fairuz Syed Mohd Dardin
Center for Tropicalization (CENTROP)
Universiti Pertahanan Nasional Malaysia
Kuala Lumpur, Malaysia
syedfairuz@upnm.edu.my

Zuhairi Abdul Rashid
Faculty of Engineering
Universiti Pertahanan Nasional Malaysia
Kuala Lumpur, Malaysia
zuhairirashid@gmail.my

Akram Abdul Aziz
Faculty of Engineering
Universiti Pertahanan Nasional Malaysia
Kuala Lumpur, Malaysia
akram@upnm.edu.my

***Abstract*— The aerodynamic design of a nose cone aircraft section is an important component in subsonic condition as it contribute to its weight and drag. The air data sensor of a fixed-wing type Unmanned Aerial Vehicles (UAV) also located on the nose cone. Thus, by focusing to the design of the nose cone the drag force of the entire aircraft body can be reduced and the flow separation can be minimized or delayed which can affect the efficiency of an aircraft. This research aims to identify the nose cone design that suitable for the air data sensor with the minimum value of drag force and observe the pressure contour of each nose cone design. Each design simulated in velocity of 10m/s, 20m/s and 30m/s with seven angles of attack from -30° to 30°. CAD software is used to design the nose cone and CFD is used to simulate the airflow as well to obtain the drag force of several design of nose cone. The original nose cone of FT Guinea Pig model and elliptical nose cone design shows the lowest value of drag coefficient compared with other proposed designs; conical and tangent ogive. The selected nose cone design will be used for implementing the air data system for the next phase of the research.**

***Keywords*— nose cone design; drag coefficient; CFD; UAV;**

I. INTRODUCTION

Unmanned Aerial Vehicles (UAV) is a technology that provides various of benefit to human kind [1], [2]. However, the limitation function of Inertial Measurement Unit (IMU) that normally used as the main sensors of the UAV to control its attitude limiting the capabilities of the UAV to fly in such harsh condition where the measurement of the drift angle is needed [3]. The concept of conventional aircraft that uses differential pressure data located on the nose cone to measure the drift angle will be implemented for UAVs. The differential pressure data also used for airspeed calculation of the UAVs. The drift angle and airspeed measurement for UAV will allow the UAV to react in crosswind conditions and still reach significant stability during maneuvering.

In this paper the UAV that being used is an off-the-shelf small fixed-wing type UAV, FT Guinea Pig (Fig. 1) by Flite Test, designed with a removable nose cone [4]. The UAV will be implemented with the air data sensor system to measure airspeed and drift angle.

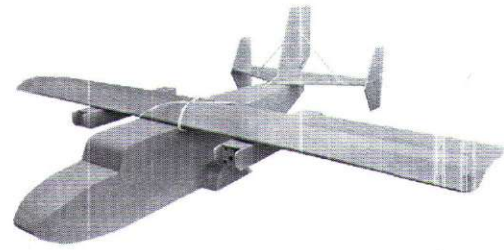

Fig. 1. FT Guinea Pig

The aim of this paper is to design a suitable nose cone of a fixed-wing type UAV that will be use to install an air data sensor system. The air data sensor system for a fixed-wing UAV consists of a pitot-static tube and flush air data sensing system (FADS) to measure the airspeed and the drift angle [5]. The pitot-static tube is used to measure the airspeed by calculating the differential pressure of the total pressure and static pressure. The pitot-static tube is a thin and long cylindrical tube shape which needs special bracket or mounting for installation. The flush air data sensing system (FADS) is a method that estimates air data parameters using pressure data collected from orifices flushed with the surface of the vehicles[5]. The system is mounted on the nose cone of the fixed-wing UAV. Thus, the design of the nose cone needs to be study thoroughly before installing the air data sensor system. The performance of the nose cone is evaluated based on the velocity streamline, pressure distribution and the drag coefficient. CFD analysis of the nose cone design is carried using ANSYS with different velocity and angle of attack.

The velocity streamline is observed to make sure the airflow around the nose cone is in laminar. The pressure distribution contour is a parameter that is used as guideline to allocate the suitable location for air data sensor system. The low value of drag coefficient of the nose cone is crucial point in subsonic aircraft as it will make decrement drag of the overall UAV. Hence this will improve the efficiency of the nose cone design.

II. Literature Review

1) Nose cone design

A comparison between various nose profile has been carried out in [6] to prove that the shape of the nose cone can postponed the boundary layer separation. The value of pressure coefficient, pressure contour and Mach contour were the parameters that are being observed. This paper concludes Von Karman ogive nose profile as the best shape for the subsonic flows as it gives the minimum pressure coefficient and higher critical Mach number than the conical, ogive and parabola shape. An analysis on various commercial aircraft nose cone profiles has been done to identify the design of nose profiles with minimum drag at specific Mach number. The velocity distribution contour and the value of drag coefficient were observed. This paper conclude that elliptical nose cone gives the minimum drag coefficient at 0.4, 0.6, and 0.8 Mach number compared to conical, parabola and ogive nose cone profiles [7]. In paper [8], the elliptical and secant ogive nose cone shape has been analyzed to study the aerodynamic characteristics. The pressure contour, velocity contour, velocity streamline and value of drag coefficient and pressure coefficient were observed. It concluded that elliptical nose cone performs better that secant ogive as the elliptical experienced less drag coefficient.

A CFD analysis of elliptical, tangent ogive, parabolic and conic nose cones have been done to analyzed the drag force generated in subsonic medium ranged from 0.05 to 0.62 of Mach number. Elliptical been concluded as the best aerodynamics shape compared to other shape [9]. A review on nose cone design for different flight regime in order to select the appropriate nose cone geometry suited with the specific flow and operating conditions has been reported in [10]. By observing the velocity contour and drag coefficient of each nose cone design, elliptical has been chosen other than parabolic and ogives shape.

Based on the review of previous research, the four models of nose cone will be analyzed in this research are the existing FT Guinea Pig, elliptical, tangent ogive and conical. The selected nose cone shape is the basic geometry figure and the geometry of each shape is discussed in the next section.

2) Geometry of the nose cone

Reference [11] describe the geometry of different nose cone design including elliptical, conical and tangent ogive where the basis of the designs is based on the geometry figures.

An elliptical nose cone is a half-ellipse. The center line (C/L) is the major axis of this design, while the base of the nose cone is the minor axis, as seen in Fig. 2. Due to its blunt tip and tangent base, this form is typically used in subsonic conditions. Equation (1) gives the radius Y at any point x varying from 0 to L.

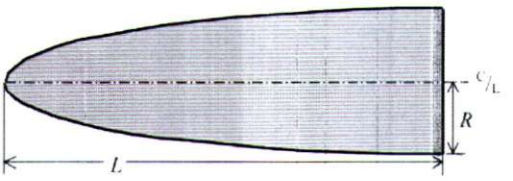

Fig. 2. Elliptical

$$Y = R\sqrt{1 - \frac{x^2}{L^2}} \tag{1}$$

Fig. 3 demonstrate the geometry of tangent ogive nose cone design where the length of the nose is the tangent to the arc of the Tangent ogive nose cone is popular in rocketry design. Equation (2) is used to compute the radius of the circle defining the ogive. The radius of the circle is ρ, while the nose cone's length is L. Since it extends from 0 to L, the equation that describes the radius at any point and defines the nose cone tangent design is presented below Fig. 3.

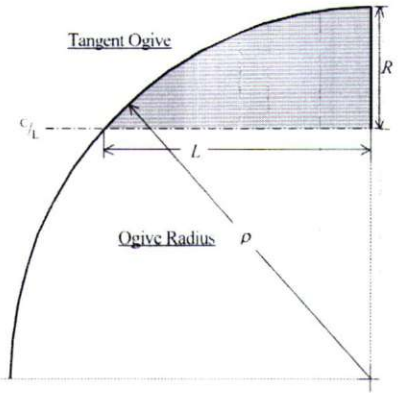

Fig. 3. Tangent ogive

$$\rho = \frac{R^2 + L^2}{2R} \tag{2}$$

Conical nose cone is the simple cone as illustrated in Fig. 4 due to it ease to manufacture and simplest in design. The equation that defines the conical design is shown in (3) and also being defined often by their sides or half angle.

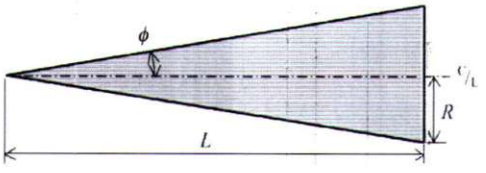

Fig. 4. Conical

$$y = \frac{xR}{L} \tag{3}$$

III. Methodology

A. Design

The three chosen nose cone shape including the design from original model nose cone are designed in SolidWork software by using the respective formulas. All of this design is based from the base-measurement that connect the nose cone with the body of the aircraft as depicted in Fig. 5 where the length and the reference area of the base of the nose cone are 0.2m and $1.69m^2$ (0.13m x 0.13m). The resulted 3D designs of the proposed nose cone are shown accordingly in Fig. 6, Fig. 7, Fig. 8 and Fig. 9

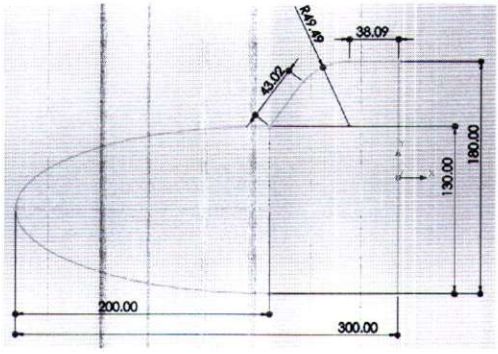

Fig. 5. The side view measurement of FT Guinea Pig nose cone in millimeter

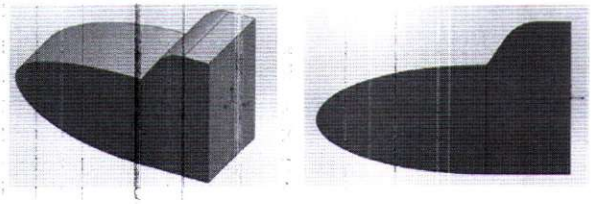

Fig. 6. FT Guinea Pig nose cone

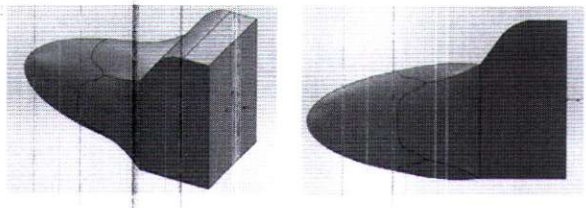

Fig. 7. Elliptical nose cone

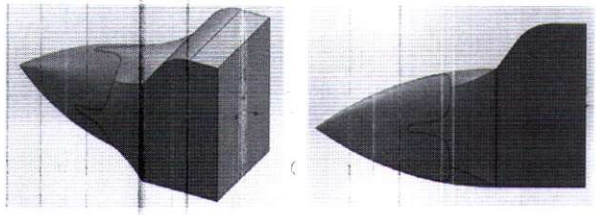

Fig. 8. Tangent ogive nose cone

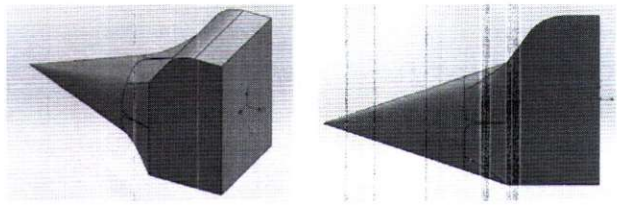

Fig. 9. Conical nose cone

B. Computational Domain

ANSYS was used to do the CFD analysis in this study which involved pre-processing, processing, and post-processing step. The designing, meshing, boundary condition, and numerical approach are all part of the pre-processing step. The processing stage entails solving the fluid flow governing equation numerically until convergence is achieved. Finally, the post-processing procedure entails extracting results in the form of graphs and contours that describe the physics of the flow, as well as the desired results.

1) Pre-processing

The four nose cone design from the SolidWork are imported to the fluent CFD in ANSYS software for meshing. For simulations, the same boundary conditions were applied to all nose cone designed where the flow velocity was 10m/s, 20m/s and 30m/s respectively. The reference values in fluent CFD are related to the value of drag coefficient and TABLE I. shows all the parameters used in the reference values and the solver used for this simulation in ANSYS was Shear Stress Transport k-ω (SST k-ω) turbulence model [12].

TABLE I. Reference Value Parameter

Reference area	FT Guinea Pig	$0.15487m^2$
	Elliptical	$0.13279m^2$
	Tangent ogive	$0.12330m^2$
	FT Guinea Pig	$0.10898m^2$
Length	0.3m	
Temperature	303.15K / 30°C	
Density	1.164	
Air viscosity	1.872×10^{-5}	

IV. Result and Discussion

The parameter of velocity streamline, pressure contour and drag coefficient are extracted form CFD post after the analysis from fluent solver. TABLE II. shows the pressure contour of FT Guinea Pig nose cone in 10m/s velocity with different angle of attacks. The same test will be applied on the rest of the nose cone designs.

TABLE II. PRESSURE CONTOUR

Angle of attack	Pressure contour
30°	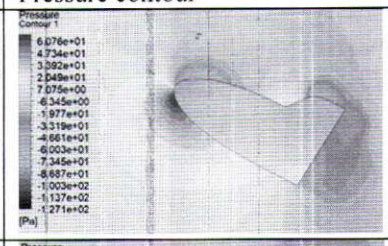
20°	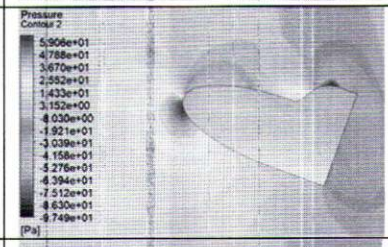
10°	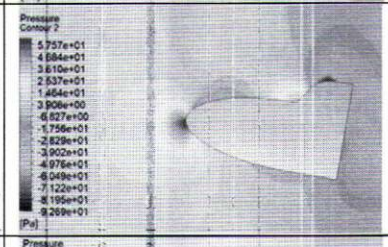
0°	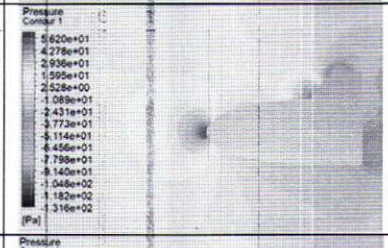
-10°	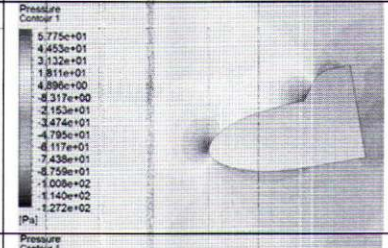
-20°	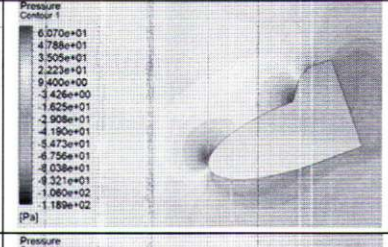
-30°	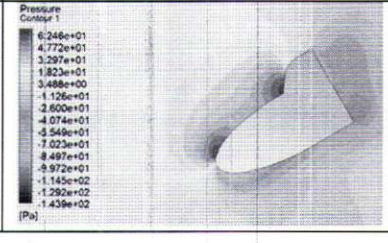

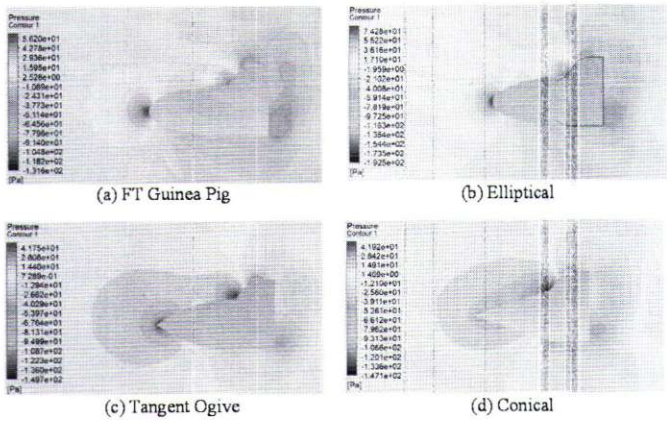

(a) FT Guinea Pig (b) Elliptical

(c) Tangent Ogive (d) Conical

Fig. 10. Pressure contour of nose cone at 10m/s, 0° angle of attack for every nose cone design

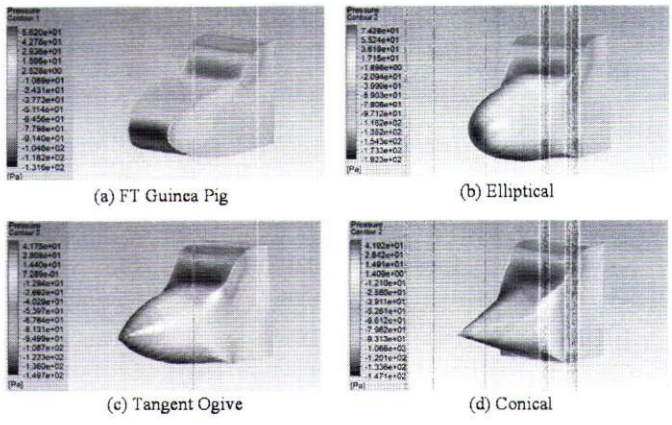

(a) FT Guinea Pig (b) Elliptical

(c) Tangent Ogive (d) Conical

Fig. 11. Pressure contour of nose at 10m/s, 0° angle of attack

Fig. 10 and Fig. 11 show the pressure contour for each nose cone design at velocity of 10m/s and 0° of angle of attack. Based on the pressure contour, the high pressure area for the FT Guinea Pig and elliptical on the tip of the nose decrease drastically along the curve line and the high pressure area are smaller compared to the tangent ogive and conical nose cone shape. The pressure contour of nose cone will be used as guideline for the next objective of the research which is defining the position of the air data sensors (pitot-static tube and static pressure port).

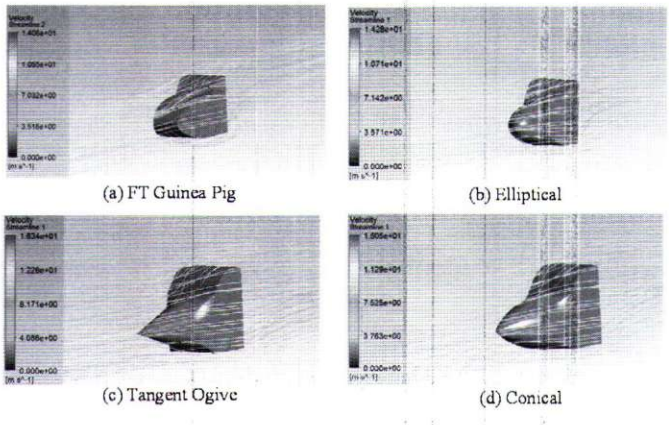

(a) FT Guinea Pig (b) Elliptical

(c) Tangent Ogive (d) Conical

Fig. 12. Velocity streamline of nose cone at 10m/s, 0° angle of attack

The Reynold number of each designed nose cone have been calculated to make sure the airflow on the nose cone is in laminar and tabulated in TABLE III. Based on the critical Reynold number for external flow, the transition from laminar to turbulence begins at around 3×10^6 [13].

TABLE III. REYNOLD NUMBER

Velocity (m/s)	Reynold number
10	1.865×10^5
20	3.731×10^5
30	5.596×10^5

Hence the airflow of all nose cone designed in this research is in laminar flow by referring to the calculated Reynold number and streamline from the simulation shown in Fig. 12 streamline of nose cone at 10m/s, 0° angle of attack. All of the nose cones experienced laminar airflow since it is in the subsonic condition. The velocity streamline is observed for the positioning of the total pressure of pitot-static tube that must be parallel with the airflow to measure the total pressure.

The value of drag coefficient of the nose cone for subsonic aircraft is important as it will determine the entire drag of the body. Thus, by obtaining lower drag coefficient on the nose cone will reducing the drag force of the entire aircraft body where the drag coefficient is defined by [14]:

$$c_d = \frac{2F_d}{\rho u^2 A} \tag{4}$$

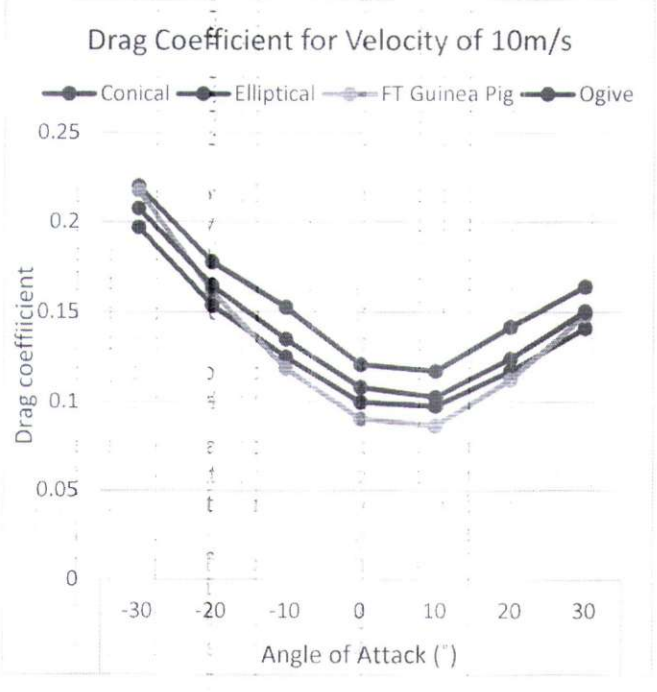

Fig. 13. Drag coefficient for velocity of 10m/s

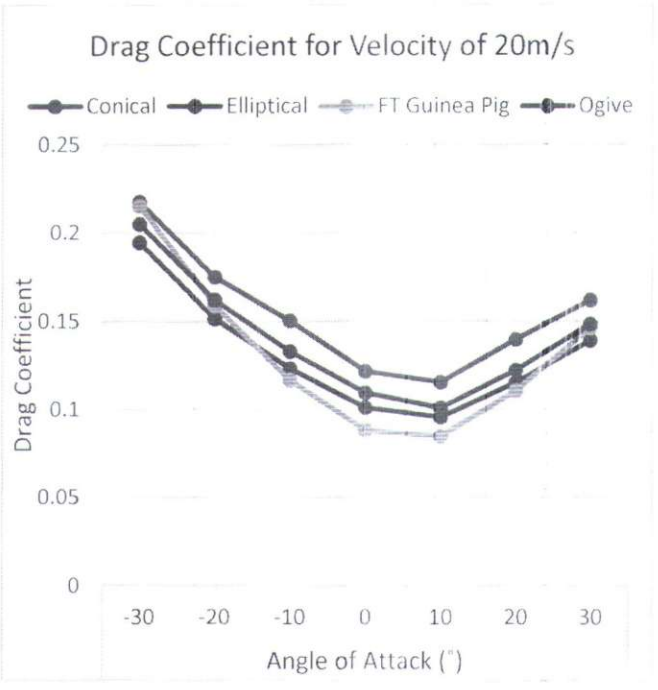

Fig. 14. Drag coefficient for velocity of 20m/s

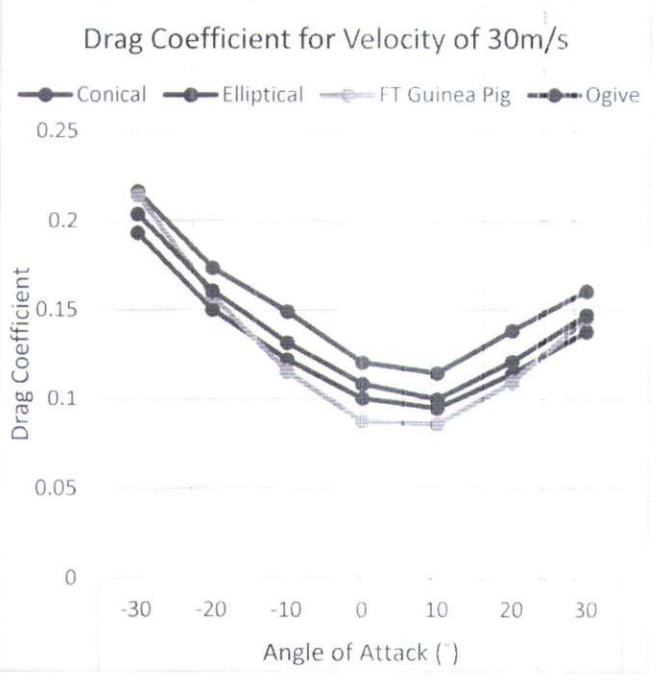

Fig. 15. Drag coefficient for velocity of 30m/s

The nose cone designs are simulated in velocity of 10m/s, 20m/s and 30m/s with different angle of attack from -30° to 30° respectively with an increment of 10° for each simulation. Based on the three figures (Fig. 13 through Fig. 15), the lowest drag coefficient of all nose cone is elliptical followed by FT Guinea Pig, tangent ogive and lastly conical.

V. Conclusion and Future Work

Based from the resulted simulation, FT Guinea Pig and elliptical nose cone shape are the most suitable shape for implementing the air data system for the UAV as both shape shows the lowest value of drag coefficient compare to tangent ogive and conical shape. The decrement of the pressure contour from the high pressure at the tip of the nose cone to low pressure also decrease drastically which resulting less high pressure area faced by the nose cone.

Based from this finding, elliptical nose cone shows the best aerodynamic performance for subsonic condition by comparing the simulation result from this finding with the simulations done in the literature review.

The next phase of the work will use the pressure contour as guideline to allocated the static pressure port of the flush air data sensing system that will help in obtaining the surface pressure distribution as it is one of the reference conditions needed. The velocity streamline also used for positioning the pitot-static tube to avoid the position error. Both pitot-static tube and static pressure port positioning will be analyzed by simulation and validate with experimental analysis in a wind tunnel.

Acknowledgment

This work is being funded by Fundamental Research Grant Scheme, Universiti Pertahanan Nasional Malaysia (UPNM), under the grant of FGRS/1/2020/TK0/UPNM/03/9.

References

[1] D. Giordan *et al.*, "The use of unmanned aerial vehicles (UAVs) for engineering geology applications," *Bull. Eng. Geol. Environ.*, vol. 79, no. 7, pp. 3437–3481, 2020, doi: 10.1007/s10064-020-01766-2.

[2] H. Shakhatreh *et al.*, "Unmanned Aerial Vehicles (UAVs): A Survey on Civil Applications and Key Research Challenges," *IEEE Access*, vol. 7, pp. 48572–48634, 2019, doi: 10.1109/ACCESS.2019.2909530.

[3] H. Tang and Z. Shen, "An Attitude Estimate Method for fixed-wing UAVs using MEMS / GPS data Fusion."

[4] "FT Guinea Pig | Flite Test." https://www.flitetest.com/articles/ft-guinea-pig (accessed Nov. 15, 2021).

[5] S. B. Vidya *et al.*, "Differential presssure based angle of attack estimation in a Flush Air Data System (FADS)," *2016 Int. Conf. Control Instrum. Commun. Comput. Technol. ICCICCT 2016*, pp. 42–48, 2017, doi: 10.1109/ICCICCT.2016.7987917.

[6] A. S. Varma, "International Journal of Aerospace and Mechanical Engineering CFD Analysis of Various Nose Profiles International Journal of Aerospace and Mechanical Engineering," vol. 3, no. 3, pp. 26–29, 2016.

[7] A. Yeshwanth and P. Senthiil, "Nose Cone Design and Analysis of an Avion," *Intenational J. Pure Appl. Math.*, vol. 119, no. 12, pp. 15581–15589, 2018.

[8] S. Chalia, "Investigation on Aerodynamic Performance of Elliptical and Secant give Nose Cones," vol. 5, no. 4, pp. 1291–1300, 2019.

[9] L. De Almeida, S. Carvalho, G. Claudino, and C. Filho, "CFD analysis of drag force for different nose cone design," no. October, 2019.

[10] A. Rajan Iyer and A. Pant, "A review on nose cone designs for different flight regimes," *Int. Res. J. Eng. Technol.*, pp. 3546–3554, 2020, [Online]. Available: www.irjet.net.

[11] G. A. Crowell Sr, "The Descriptive Geometry of Nose Cones," *Tech. Data*, p. 15, 1996.

[12] ANSYS, "Introduction to ANSYS Fluent," *ANSYS Cust. Train. Mater.*, no. December, pp. 1–59, 2010.

[13] C. A. Yunus and J. G. Afshin, *Heat and Mass Transfer: Fundamentals & Applications*, Fifth. New York: McGraw-Hill Education, 2015.

[14] M. Bakirci, "Design and Aerodynamic Analysis of a Rocket Nose Cone with Specific Fineness Ratio," pp. 80–85, 2021, doi: 10.1109/apuavd53804.2021.9615407.